# Measurements of Fusion Cross Sections in the Systems $^{10,14,15}$C + $^{12}$C with a Multi-sampling Ionization Chamber

P. F. F. Carnelli,[1,2,3] S. Almaraz-Calderon,[1] K. E. Rehm,[1] M. Albers,[1] M. Alcorta,[1,*] P. F. Bertone,[1,†] B. Digiovine,[1] H. Esbensen,[1] J. O. Fernández Niello,[2,4] D. Henderson,[1] C. L. Jiang,[1] J. Lai,[5] S. T. Marley,[1,‡] O. Nusair,[1] T. Palchan-Hazan,[1] R. C. Pardo,[1] M. Paul,[6] and C. Ugalde[1]

[1]*Physics Division, Argonne National Laboratory, Argonne, Illinois 60439, USA*
[2]*Laboratorio Tandar, Comisión Nacional de Energía Atómica, B1650KNA San Martín, Buenos Aires, Argentina*
[3]*Consejo Nacional de Investigaciones Científicas y Técnicas, C1033AAJ Buenos Aires, Argentina*
[4]*Escuela de Ciencia y Tecnología, Universidad de San Martín, B1650BWA San Martín, Buenos Aires, Argentina*
[5]*Department of Physics and Astronomy, Louisiana State University, Baton Rouge, Louisiana 70803, USA*
[6]*Racah Institute of Physics, Hebrew University, Jerusalem, Israel, 91904*

(Dated: February 6, 2014)

The interaction between neutron-rich nuclei plays an important role for understanding the reaction mechanism of the fusion process as well as for the energy production through pycnonuclear reactions in the crust of neutron stars. We have performed the first measurements of the total fusion cross sections in the systems $^{10,14,15}$C + $^{12}$C using a new active target-detector system. In the energy region accessible with existing radioactive beams a good agreement between the experimental and theoretical cross sections is observed. This gives confidence in our ability to calculate fusion cross sections for systems which are outside the range of today's radioactive beam facilities.

PACS numbers: 25.60.Pj, 26.30.-k, 26.60.Gj
Keywords:

Fusion reactions are central in our attempts to produce and study exotic nuclei away from the valley of stability. By bombarding targets with beams of heavy ions we have generated nuclei located at and beyond the proton-drip line and extended the periodic table towards new superheavy elements [1]. In all these experiments it is important to have a good understanding of the underlying reaction mechanism. For that reason a large number of heavy-ion induced fusion reactions have been studied during the last three decades. These studies have revealed that the underlying reaction dynamics is more complex than expected by just assuming the formation of a compound nucleus starting from a di-nuclear configuration at the interaction barrier. It was found that intrinsic excitations of the target or projectile can critically affect the fusion process, which led to the development of coupled-channels descriptions including inelastic and transfer channels. These coupled-channel effects were found to enhance the fusion cross section by several orders of magnitude at sub-barrier energies. Most of these studies have been performed using stable beams. The availability of radioactive beams has opened the possibility to also study fusion reactions induced by halo nuclei *i.e.* nuclei with weakly bound neutrons or protons, which can also lead to a considerable increase in the fusion probablity at low energies [2].

Fusion reactions also play an important role in nuclear astrophysics. The $^{12}$C + $^{12}$C fusion reaction is an important energy source during the late stages of stellar evolution and in stellar explosions such as type Ia supernovae and in X-ray bursts [3]. X-ray bursts, *i.e.* a sudden increase in X-ray intensity emitted by a neutron star, occur in binary systems when the neutron star accretes hydrogen and helium material from a companion 'donor' star. When enough material has been accumulated it ignites in a thermonuclear explosion converting the hydrogen and helium fuel into exotic proton-rich nuclei via the rapid proton capture (rp) process. Typical X-ray bursts have rise times between 1-10 sec and last about 10-100 sec and release about $10^{39-40}$ ergs. The ashes from these thermonuclear explosions then move deeper into the 'ocean' of the neutron star where electron capture reactions can lead to a lowering of their atomic numbers. The resulting neutron-rich nuclei play a crucial role in the so-called superbursts which are thought to occur in the vicinity of the neutron star crust [4]. Although details of this process are still being debated, several calculations of fusion cross sections between neutron-rich carbon ($^{24}$C + $^{24}$C), oxygen ($^{24}$O + $^{24}$O) and neon ($^{40}$Ne + $^{40}$Ne) nuclei have recently been published [5–7]. Most of the reactions included in these calculations are outside the range of our current experimental capabilities. A first experimental attempt has been made to study fusion reactions involving neutron-rich nuclei, using a $^{20}$O beam from the SPIRAL facility for a measurement of the fusion cross section in the system $^{20}$O on $^{12}$C [8, 9]. Due to the detection system, however, only the cross sections associated with charged-particle emission could be extracted in this experiment.

Studies of fusion reactions with secondary ion beams

suffer from low beam intensities available at today's radioactive beam facilities. In order to measure a range of an excitation function in one step, different techniques have been used in the past, such as bombarding a stack of target foils with low-intensity beams, followed by off-line measurements of the resulting radioactivities through $\alpha, \beta$, or $\gamma$ counting [10, 11]. However, these techniques require reaction products with suitable properties (half lives, decay channels, *etc.*) and put severe restrictions on the experiments.

In this publication we describe the first measurement of the total fusion cross sections of $^{10,14,15}$C + $^{12}$C, ranging from neutron-deficient $^{10}$C to 'neutron-rich' $^{15}$C using a new active target-detector system. The technique makes use of a so-called MUlti-Sampling Ionization Chamber (MUSIC) filled with $CH_4$ gas serving both as target and counting gas. Multi-sampling ionization chambers have been used in the past in experiments with relativistic heavy ions [12, 13] and a similar detector was employed in a measurement of the $^8$Li($\alpha$,n)$^{11}$B reaction [14, 15]. To our knowledge this is the first application of this technique for measurements of fusion reactions with radioactive beams. The technique used in our experiment is similar to the one discussed in Ref. [14]. Details will be published in a separate paper [16].

The anode of the detector is subdivided into 18 strips as shown in the bottom part of Fig. 1. The two anode signals ($E_0$ and $E_{17}$) at the beginning and the end of the chamber were used as veto signals to eliminate events occurring in the entrance and exit windows. A radioactive beam, *e.g.*$^{15}$C with an energy of 49 MeV, entering the ion chamber through a 1.45 mg/cm$^2$ Ti window experiences an energy loss in the gas volume at each of the 18 anode strips corresponding to about 1.4 MeV per strip at a $CH_4$ pressure of 200 mbar, thus, sampling the C + C fusion reaction in the center-of-mass energy range $E_1$=18 MeV to $E_{16}$=9 MeV. The signals measured for these beam-like events are shown by the black traces in Fig. 1. A fusion reaction occuring in the gas volume at one of the anode strips (e.g. strip 4, see lower part of Fig. 1) is identified by beam-like energy losses in strip 0-3, followed by larger signals generated by the C + C evaporation residues in the following 3-5 strips and no signal in the remaining strips as indicated by the red lines in Fig. 1. In order to discriminate against elastic or inelastic scattering events, the anode strips 1-16 are subdivided into two parts (marked L and R in the lower part of Fig.1) which are used as a multiplicity filter. While beam-like or fusion events have multiplicity one (*i.e.* signals that occur either in the right or the left side of the anode strips), elastic and inelastic scattering produces multiplicity 2 events that can easily be rejected using the 'beam-right' and 'beam-left' information.

Beams of the short-lived isotopes $^{10}$C ($t_{1/2}$=19.3 s) and $^{15}$C($t_{1/2}$=2.45 s) were generated at the ATLAS accelerator with the In-Flight Technique using primary beams

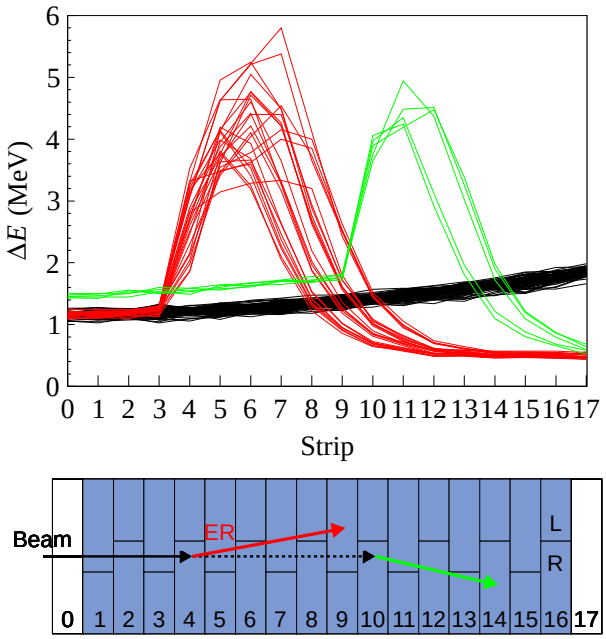


FIG. 1: (Color online) Top: Energy loss signals from the Multi-Sampling Ionization Chamber (MUSIC) for various reactions induced by $^{15}$C and $^{15}$N particles. Black: Energy-loss signals measured in the 18 strips for $^{15}$C beam particles passing through the MUSIC detector. Red: Energy-loss values measured for evaporation residues (ER) produced by $^{15}$C particles in anode strip 4. Green: Energy-loss values measured for evaporation residues produced by $^{15}$N particles in anode strip 10. Bottom: Schematic of the anode structure. See text for details.

of $^{10}$B and $^{14}$C and the inverse reactions $^1$H($^{10}$B,$^{10}$C)n and $^2$H($^{14}$C,$^{15}$C)$^1$H, respectively. The beams were transported to the MUSIC detector through a 26° bending magnet and a RF sweeper system which eliminated most of the scattered primary beam particles. Details of the In-Flight Technique can be found in Ref. [17]. For the production of a $^{14}$C beam ($t_{1/2}$=5730 y) a $^{14}$C sample was mounted in the negative-ion sputter source of the tandem accelerator at Argonne National Laboratory. The energy of the carbon beams was typically between 40-50 MeV.

Besides the low intensities, the beam purity is another difficulty in experiments with radioactive beams since they are produced via two-step processes. While for the production of a $^{15}$C$^{6+}$ beam via the $^2$H($^{14}$C,$^{15}$C)p reaction, interferences from the primary $^{14}$C$^{6+}$ particles can be reduced using a RF sweeper, the contributions from $^{15}$N$^{6+}$ particles from the $^2$H($^{14}$C,$^{15}$N)n reaction cannot be eliminated. However, the higher energy loss of the $^{15}$N particles in the MUSIC detector prior to the fusion event (see green curves in Fig. 1) allowed us to separate events from $^{15}$N-induced fusion reactions. In addition, the timing signal from the cathode has been used to eliminate events caused by beam contaminants from the production beam, which arrive at different times at the detector. In

order to eliminate pileup in the ionization chamber, the beam was pulsed with a repetition time of 8 $\mu$sec which was long enough to allow the electrons generated in the ion chamber to drift to the Frisch grid. The response of the MUSIC detector to these various reactions was tested using Monte Carlo simulations and found to be in good agreement with the experimental data shown in Fig. 1.

The energy loss of carbon ions in methane and the entrance and exit windows was determined using well-collimated carbon beams with known energies passing through the MUSIC detector. The detector was filled with $CH_4$ at different pressures and the transmitted carbon ions were detected in a magnetic spectrograph located after the ion chamber. A comparison of the experimental energies with various energy-loss tables from the literature [18, 19] showed that the best agreement was obtained with the tables from Ref. [19]. This allowed us to determine the average energy of the incident beams in the middle of each anode strip.

An advantage of a multi-sampling ionization chamber for measurements of fusion reactions is the good absolute beam normalization. With traditional techniques each measurement at a given energy has to be normalized with a monitor detector to the individual beam dose which can introduce additional (statistical and systematic) uncertainties. In this new approach the beam dose is the same for all anode strips (i.e. all energies) and the number of incident beam particles is measured under the same conditions as the fusion events.

In order to test this new active target system we have re-measured the fusion cross sections of the stable systems $^{12,13}$C + $^{12}$C for which high-precision data can be found in the literature [20, 21]. To simulate the intensities expected in experiments with radioactive beams and to ensure that there was only one particle in each beam pulse, the $^{12,13}$C beam intensities were reduced to rates of about 5x10$^3$ particles/sec. The running time for each beam-target combination in these experiments was about 18 hours. In a second step we measured the fusion between beams of the radioactive ions $^{10,14,15}$C and $^{12}$C at energies around the Coulomb barrier. These data were then used to test the ability of theoretical calculations to reproduce the experimental results.

The fusion cross sections for $^{10,12,13,14,15}$C on $^{12}$C converted into astrophysical S factors are shown by the solid points in Fig. 2. The solid lines are calculations by Yakovlev *et al.* [6] which are based on tunneling calculations using the Sao Paulo potential. The red circles are S factors for the systems $^{12,13}$C + $^{12}$C for which data in the energy range from about 3 to 30 MeV are available [20, 21]. Also shown are the theoretical predictions for the system $^{19}$C + $^{12}$C which is the heaviest carbon isotope that is predicted to be available at the next generation FRIB facility with beam intensities exceeding 10$^3$ particles/sec. A very good agreement of our data with the earlier measurements of Ref. [20, 21] for $^{12,13}$C is

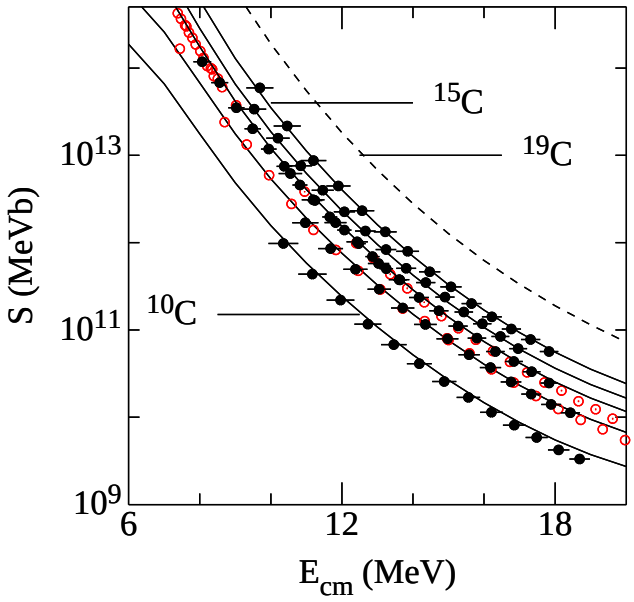


FIG. 2: (Color online) Solid points: Experimental data for the S factors in the fusion reactions $^{10,12,13,14,15}$C + $^{12}$C as measured with the MUSIC detector. Open circles: Experimental data for $^{12,13}$C + $^{12}$C from Refs. [20, 21]. Solid lines: Theoretical S factors for the systems $^{10,12,13,14,15}$C + $^{12}$C taken from the calculations of Yakovlev *et al.* [6]. Dashed line: Theoretical S-factor for the system $^{19}$C + $^{12}$C.

observed. The energy dependence of the data is also well described by the predictions of Yakovlev et al. [6] especially in the energy range $E_{cm} \leq 14$ MeV. At the highest energies shown in Fig. 2 deviations between theory and experiment can be seen.

To show this in more detail we have plotted in the top part of Fig. 3 the fusion cross section for the systems $^{10,12,13,14,15}$C + $^{12}$C (red points) measured in this experiment, averaged over the energy range E$_{cm}$=14-17 MeV as a function of the neutron excess N-Z. Also shown are the fusion cross sections for the stable isotopes $^{12,13}$C (red circles), $^{14,15}$N (triangles) and $^{16,17,18}$O (squares) + $^{12}$C taken from Ref. [20]. No other cross section data for fusion with radioactive carbon isotopes are available in this energy range. The data are plotted as reduced cross sections, defined as $\sigma_{reduced} = \sigma/(\pi R^2)$, where $R = 1.2(A_P^{1/3} + A_T^{1/3})$ and $A_P$ and $A_T$ are the masses of projectile and target, respectively. This conversion takes standard geometrical size effects into account. Nevertheless the fusion cross sections for the carbon isotopes experience an additional 20% increase going from $^{10}$C to $^{15}$C. A similar increase is observed for fusion of $^{12}$C with the neighboring stable nitrogen and oxygen isotopes. For these elements, however, the increase occurs in one step going from the $N - Z$=0 to the $N - Z$=1 isotopes.

A comparison between theoretical and experimental fusion cross sections for $^{10,12,13,14,15}$C + $^{12}$C is shown in the lower part of Fig. 3. The solid line is the pre-

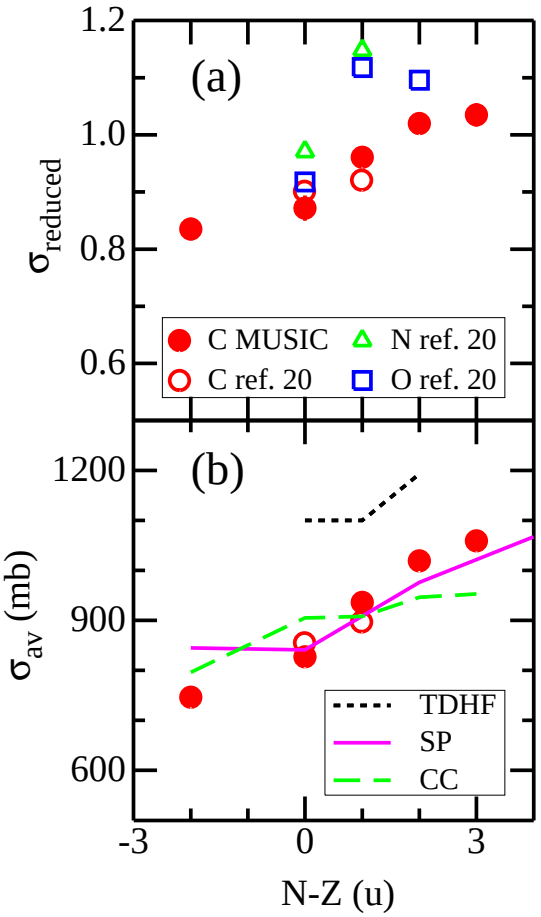


FIG. 3: (Color Online) (a) Solid points: Reduced cross sections (see text for details) averaged in the energy range $E_{cm}$=14-17 MeV for the fusion reactions $^{10,12,13,14,15}$C + $^{12}$C as measured with the MUSIC detector and plotted as function of the neutron excess $N - Z$. Open symbols: Experimental data for $^{12,13}$C + $^{12}$C (red circles), $^{14,15}$N + $^{12}$C (green triangles) and $^{16,17,18}$O + $^{12}$C (blue squares) from Ref. [20]. (b) Comparison of the experimental averaged cross sections for $^{10,12,13,14,15}$C + $^{12}$C (circles) with theoretical predictions: solid line: cross- sections prediction taken from the calculations of Yakovlev *et al.* [6], dashed line: cross section predicted by coupled-channel calculations from Ref. [24], dotted line: cross section predicted by TDHF calculations [23].

diction of Yakovlev et al. [6], which in the mass range $^{12}$C-$^{15}$C agrees with the data to better than 4%,but overpredicts the cross sections for $^{10}$C + $^{12}$C by about 13%. The dashed line is the prediction of coupled-channel calculations by Esbensen *et al.* [24] which include couplings to one- and two-phonon excitations as well as mutual quadrupole and octupole excitations in projectile and target. These cross sections are also in good agreement (better than 10%) for all carbon isotopes (including $^{10}$C) with a somewhat shallower slope of $\sigma_{av}$ towards the heavier carbon isotopes. The dotted curve for $^{12,13,14}$C ($N - Z$=0,1,2) is the result of a TDHF calculation from Umar *et al.* [23]. These values are generally larger than the experimental cross sections, due to the fact that TDHF calculations describe the sum of fusion and transfer channels.

It has been argued that the dynamics of the neutron-rich skin might lead to an enhancement of the fusion cross sections [25]. While this has been found e.g. in the fusion of $^{15}$C + $^{232}$Th [26] at energies in the vicinity of the Coulomb barrier, no effect has been seen in the interaction cross sections obtained from high-energy C + C scattering of Ref. [27].

The good agreement between theoretical predictions and experimental data is very encouraging. Fusion reactions occurring in the crust of neutron stars such as $^{24}$C + $^{24}$C will remain outside of our experimental capabilities for the foreseeable future. Comparisons between theory and experiment like the one presented here allow us to calibrate the calculations for cases that can not be studied in the laboratory.

In summary, we have performed the first measurements of the fusion cross sections between $^{12}$C and the radioactive isotopes of $^{10,14,15}$C and compared their systematic behavior as a function of neutron number with neighboring systems and with different kinds of calculations. The measurements were performed with a new, high-efficiency technique using a multi-sampling ionization chamber with a segmented anode which allows us to determine in a single measurement a large part of the excitation function, thus, eliminating difficulties with the relative normalization of the cross sections. Test experiments with stable $^{12,13}$C beams are in excellent agreement with data from the literature. The measured cross sections are of interest to nuclear astrophysics where in the crust of accreting neutron stars neutron-rich isotopes are thought to undergo pycnonuclear fusion reactions. A comparison between the data and theoretical calculations have shown a good agreement with tunneling calculations using the Sao Paulo potential and with coupled-channels calculations if couplings to two-phonon excitations are included. The high efficiency of this active detector system will allow future measurements with even more neutron-rich isotopes. By using other gases (e.g. $^{4}$He,$^{13}$CH$_4$, Ne, Ar, Kr) excitation functions of other reactions involving radioactive beams can be measured as well.

We want to thank S. Umar for providing us with the TDHF cross sections in tabulated form. This work was supported by the US Department of Energy, Office of Nuclear Physics under contract No. DE-AC02-06CH11357, the Consejo Nacional de Investigaciones Científicas y Técnicas (CONICET), Argentina and the Universidad Nacional de San Martín Grant SJ10/39.

* Present address: TRIUMF, Vancouver, British Columbia, VGT 2A3, Canada

† Present address: Marshall Space Flight Center, Huntsville, Alabama 35812, USA
‡ Present address: Department of Physics, University of Notre Dame, Notre Dame, Indiana 46556, USA

[1] B. B. Back, H. Esbensen, C. L. Jiang and K. E. Rehm, Rev. Mod. Phys. in print (2014).
[2] J. F. Liang and C. Signorini, Int. J. Mod. Phys. **E14**, 1121 (2005).
[3] G. Wallerstein *et al.*, Rev. Mod. Phys. **69**, 995 (1997).
[4] A. Cumming and L. Bildsten, Astrophys. J. **559**, L127 (2001).
[5] C. J. Horowitz, H. Dussan and D. K. Berry, Phys. Rev. C **77**, 045807 (2008).
[6] D. G. Yakovlev, M. Beard, L. R. Gasques and M. Wiescher, Phys. Rev. C **82**, 044609, 2010. M. Beard *et al.*, At. Data Nucl. Data Tables **96**, 541 (2010).
[7] A. S. Umar, V. E. Oberacker and C. J. Horowitz, Phys. Rev. C **85**, 055801 (2012).
[8] M. J. Rudolph *et al.*, Phys. Rev. C **85**, 024605 (2012).
[9] R. T. de Souza, S. Hudan, V. E. Oberacker and A. S. Umar, Phys. Rev. C **88**, 014602 (2013).
[10] A. Lemasson *et al.*, Phys. Rev. Lett. **103**, 232701 (2009).
[11] A. Lemasson *et al.*, Phys. Lett. B **697**, 454 (2011).
[12] W. B. Christie *et al.*, Nucl. Instr. Meth. Phys. Res., Sect. A **255**, 466 (1987).
[13] K. Kimura *et al.*, Nucl. Instr. Meth. Phys. Res., Sect.A **297**, 190 (1990).
[14] R. N. Boyd *et al.*, Phys. Rev. Lett. **68**, 1283 (1992).
[15] Y. Mizoi *et al.*, Nucl. Instr. Meth. Phys. Res., Sect.A **431**, 112 (1999).
[16] P. F. F. Carnelli *et al.* Nucl. Instr. Meth. Phys. Res., Sect.A, to be published.
[17] B. Harss *et al.*, Rev. Sci. Instrum. 71, 380 (2000).
[18] J. F. Ziegler et al., Nucl. Inst. Meth., Sect. B **268**, 1818 (2010), www.srim.org.
[19] O. B. Tarasov and D. Bazin, Nucl. Instr. Meth., Sect. B **266**, 4657 (2008), lise.nscl.msu.edu.
[20] D. G. Kovar *et al.*, Phys. Rev. C **20**, 1305 (1979).
[21] R. A. Dayras, R. G. Stokstad, Z. E. Switkowski, and R. M. Wieland, Nucl. Phys. A **265**, 153 (1976).
[22] C. L. Jiang *et al.*, Phys. Rev. Lett. **110**, 072701 (2013).
[23] S. A. Umar, private communication.
[24] H. Esbensen, X. D. Tang and C. L. Jiang, Phys. Rev. C **84**, 064613 (2011).
[25] A. S. Umar, V. E. Oberacker and C. J. Horowitz, Phys. Rev. C **85**, 055801 (2012).
[26] M. Alcorta *et al.*, Phys. Rev. Lett. **106**, 172701 (2011).
[27] A. Ozawa *et al.*, Nucl. Phys. A **691**, 599 (2001).